Int J Clin Exp Pathol 2019;12(2):640-656
www.ijcep.com /ISSN:1936-2625/IJCEP0088243

Original Article

GSK-3β mediates ischemia-reperfusion injury by regulating autophagy in DCD liver allografts

Tingting Liu[1,3], Yang Han[2], Wu Lv[4], Pan Qi[1,3], Wenshi Liu[1,3], Ying Cheng[1,3], Jianan Yu[1,3], Yongfeng Liu[1,3]

[1]Department of Hepatobiliary Surgery of No. 1 Hospital of China Medical University, Shenyang, Liaoning, PR China; [2]Department of Pathology of No. 1 Hospital of China Medical University, Shenyang, Liaoning, PR China; [3]The Key Laboratory of Organ Transplantation in Liaoning, Shenyang, Liaoning, PR China; [4]Department of General Surgery, Cancer Hospital of China Medical University, Liaoning Cancer Hospital and Institute, Number 44 Xiaoheyan Road, Dadong District, Shenyang 110042, Liaoning Province, PR China

Received November 11, 2018; Accepted December 20, 2018; Epub February 1, 2019; Published February 15, 2019

Abstract: To elucidate the role of autophagy in ischemia-reperfusion injury (IRI) and determine whether glycogen synthase kinase-3β (GSK-3β) plays an important role in autophagy, a donors of cardiac death (DCD) liver transplantation model was established to observe the expression of GSK-3β and autophagy in hepatocytes during liver IRI. Immunohistochemical staining and western blotting were used to detect expression of the autophagy markers, LC3 and p62, as well as study the expression of GSK-3β and AMPK. Serum enzymology changes were analyzed at different times after liver transplantation. Hypoxia-reoxygenation methods were used to mimic the process of ischemia-reperfusion injury in cultured hepatocytes. In DCD liver transplantation with a prolonged reperfusion time, LC3 expression increased, whereas p62 decreased. GSK-3β and AMPK expression in the transplanted liver tissue were consistent with changes in autophagy, ALT, and AST. In summary, inactive GSK-3β reduced liver IRI, promoted hepatocyte autophagy, and improved hepatocyte activity. Therefore, GSK-3β may regulate autophagy through the AMPK-mTOR pathway.

Keywords: DCD liver transplantation, ischemia-reperfusion injury, GSK-3β, autophagy

Introduction

Ischemia-reperfusion injury (IRI) is the main cause of intrahepatic biliary disease and graft loss following liver transplantation. Some studies have shown that autophagy is reduced after cold/warm IRI [1-3], while others indicate increased autophagy in liver cells [4-8]. Glycogen synthase kinase-3β (GSK-3β) plays an important role in a variety of signal transduction pathways, such as embryo development, cellular differentiation, apoptosis, tumor formation, and hepatocyte protection; however, the mechanism by which GSK-3β regulates autophagy remains unclear [9-11]. Moreover, the expression of autophagy markers in liver transplantation IRI and whether GSK-3β plays an important role in hepatocyte autophagy remains unknown. If GSK-3β can regulate autophagy to further reduce IRI, then GSK-3β may be a novel target to improve the prognosis of transplant patients. This study attempted to observe the changes in GSK-3β expression and hepatocyte autophagy during IRI following liver transplantation in both small and large animals.

Materials and methods

Animal and groups

A DCD liver transplantation model was established in both small and large animals. A total of 25 pairs of specific pathogen free (SPF) male Sprague Dawley rats weighing 220 g-310 g were used as a small animal model. The body weight of the recipients was slightly heavier than that of the donors. A total of 25 DCD liver transplantations were performed [12-17]. The portal vein blood transfusion time was divided into 0-h, 3-h, 6-h, 12-h, and 24-h groups, with five pairs in each group. Each group of recipient rats was sacrificed by anesthesia at the indicated time after surgery, venous blood was collected, and the liver tissue samples were transplanted. Five normal control rats were also set

up to collect venous blood and liver tissue samples after anesthesia. The animals were fasted for 12 h before surgery and deprived of water for 8 h.

For the large animal model, 10 pairs of male or female healthy Bama miniature pigs aged 4 to 6 months and weighing 22 kg to 34 kg were used. The weight of the recipients was slightly heavier than that of the donors, and a total of 10 DCD liver transplantations were performed [18, 19]. The portal vein blood transfusion time was divided into 0-h, 3-h, 6-h, 12-h, and 24-h groups. Transplanted liver tissue and venous blood samples were collected. Donor liver tissue and recipient venous blood were collected as the normal control group. The animals were fasted for 24 h and deprived of water for 8 h before surgery.

Animal ethics standards

Human normal hepatocytes (L02 hepatocytes) were purchased from the cell bank of the Institute of Basic Medical Sciences, Chinese Academy of Medical Sciences. In accordance with the experimental conditions, they were divided into the control, autophagy activator (positive control group), blank plasmid vector transfected (Vector), wild-type GSK-3β plasmid transfected (GSK-3β-Wt), and inactivated GSK-3β plasmid transfected (GSK-3β-K85R), and transfection-activated GSK-3β plasmid (GSK-3β-S9A groups).

Establishment of rat DCD liver transplantation model

The inferior vena cava on the liver was anastomosed using the "magnetic ring method" [20]. The portal vein and inferior vena cava under the liver were reconstructed using the "double cuff technique" [17]. The magnetic ring was a gift from the Tianjin First Central Hospital.

Establishment of DCD liver transplantation model in bama miniature pigs

The following vascular and biliary tract reconstruction methods were employed: classic orthotopic liver transplantation; anastomosis of the inferior vena cava on the liver; portal vein; inferior vena cava under the liver; hepatic artery; and intubation anastomosis of the bile duct.

Immunohistochemical staining

Analysis of the immunohistochemical staining results was performed as follows: five fields were randomly selected from each slice, and 100 hepatocytes were counted in each field. Based on the percentage of the counted cell coloration, the percentage of the expression of the four proteins was divided into five levels: 0 points (no coloring); 1 point (< 25%); 2 points (< 50%); 3 points (< 75%); and 4 points (> 75%). According to the cell staining intensity the expression of the four proteins was divided into three levels: 0 points (no coloring); 1 point (light yellow particles); and 2 points (dark yellow or tan particles). Each tissue slice corresponds to a percentage and a coloring score, and the result of the multiplication is the final score of the slice.

Western blot analysis of the expression of LC3, p62, and AMPK in the liver

Electrophoresis was performed on a spacer gel at 90 V, when the sample reached the separation gel, the voltage was adjusted to 100 V. The time for electrophoresis was approximately 2 h (the gel was stopped based on the position of the pre-stained rainbow marker band).

The proteins were transferred to PVDF membranes (LC3: 60V for 30 min; AMPK: 70V for 75 min; p62 70V for 75 min; β-actin: 60V for 60 min).

The secondary antibody was added to the culture dish (10 mL, 1:1000 diluted with TBST).

Gel image analysis

The optical density values were analyzed with a gel image processing system, and the grayscale values of the bands were measured. The ratio with actin was used to calculate the relative expression levels. The experiment was repeated three times to obtain the mean value. A *t*-test was performed on the ratio of the detected value compared to the control group, and a threshold of $P < 0.05$ was considered significant.

Serum enzymology

The collected venous blood was centrifuged to obtain a supernatant, and an automatic bio-

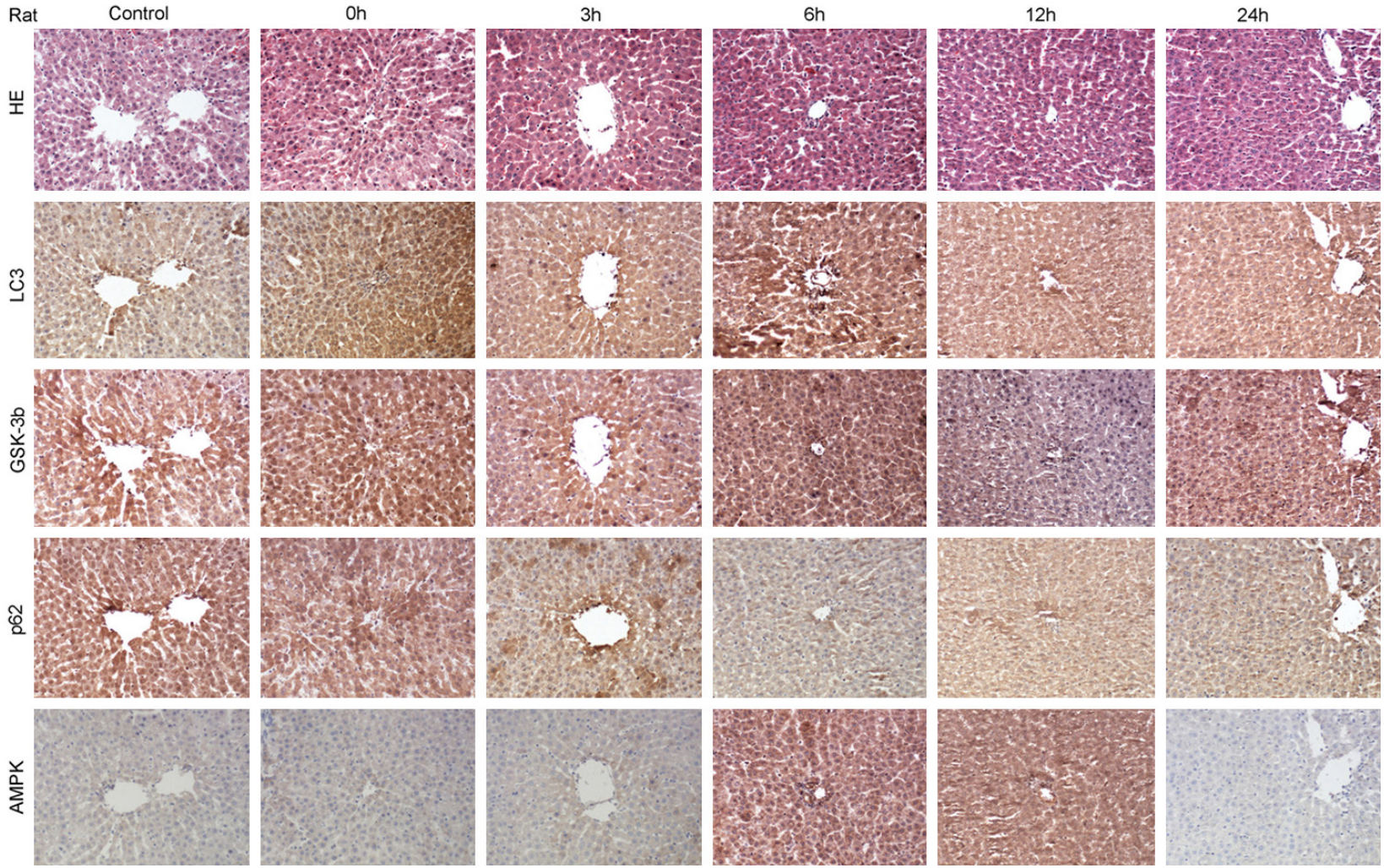

Figure 1. The hepatic changes in H&E and immunohistochemical stained (LC3, GSK-3β, p62 and AMPK) samples at different time points following liver transplantation in rats (×200).

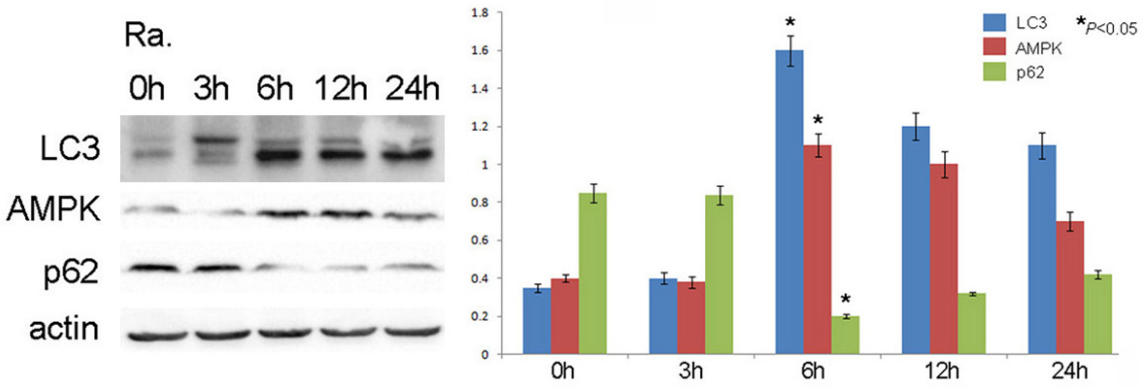

Figure 2. Western blot detection of LC3, p62, and AMPK expression in liver tissue. The expression of LC3, p62, and AMPK in the 6 h group was significantly different from the other groups. *P < 0.05 indicates statistical significance.

chemical analyzer was used to detect the serum hepatic functional enzymology. ALT (alanine aminotransferas), AST (aspartate aminotransferase), ALP (alkaline phosphatase), GGT (γ-glutamyl Transpeptidase), TP (total protein), ALB (albumin), and TBIL (total bilirubin) were detected in the rat serum; ALT, AST, ALP, GGT, and TBIL were detected in the pig serum.

Cell culture

RPMI-1640 medium was used to culture the L02 cells at 37°C in a 5% CO_2 incubator. The medium was changed every other day. When the L02 cells were in the logarithmic growth phase, they were used for experiments.

Transfection of cells

Plasmid Construction: Plasmid pCDNA3.0 GSK-3β-V5 was kindly provided by Professor Thilo Hagen of the University Nottingham, UK. This plasmid contained the insertion of a GSK-3β open reading frame between XbaI and KpnI in the pCDNA3.0 vector with a V5 tag gene. The plasmid was approximately 1300 bp. Three plasmids were constructed: 1) highly expressed GSK-3β (GSK-3β-Wt); and 2) structurally activated GSK-3β (GSK-3β-S9A); and 3) kinase-inactive GSK-3β (GSK-3β-K85R). The plasmid sequencing was validated by Dalian Takara (Bao Biomedical Technology Co., Ltd).

Transfection: The cells were transiently transfected using Lipofectamine 3000 according to the manufacturer's instructions. After 48 h, an anaerobic-reoxygenation culture was performed to simulate hepatocyte ischemia-reperfusion injury.

Hepatocyte anaerobic-reoxygenation culture

After the cells were transfected with GSK-3β-Wt, GSK-3β-S9A, GSK-3β-K85R, or the vector plasmid for 48 h, the cells were placed in an anaerobic incubator and an oxygen-free gas mixture (10% H_2, 10% CO_2, 80% N_2) was added. The cells were cultured anaerobically for 8 h, then removed and placed in a 37°C cell incubator at 5% CO_2 for 4 h for reoxygenation. L02 liver cells were subjected to anaerobic-reoxygenation culture as a blank control according to the same method described above. For the autophagy activator (positive control) group, 25 μM rapamycin was added to the L02 hepatocytes, and an anaerobic-reoxygenation culture was performed after 48 h according to the method described above.

Cell Immunofluorescence assay

The samples were incubated with the primary antibody (diluted antibody in PBS, LC3 1:200, p62:200, AMPK 1:200) at 4°C overnight. The stained samples were observed and images were taken using a fluorescence microscope. The fluorescence intensity and area were analyzed with Image ProPlus software. There was a significant difference between $P < 0.05$.

MTS assay

An MTS assay was used to detect the effects of GSK-3β on L02 hepatocyte activity. Autophagy activators were added, or the cells were transfected with GSK-3β-Wt, GSK-3β-K85R, GSK-3β-S9A, or blank plasmids. The control group did not receive any treatment. The cells were incubated in a 5% CO_2 incubator at 37°C for 48

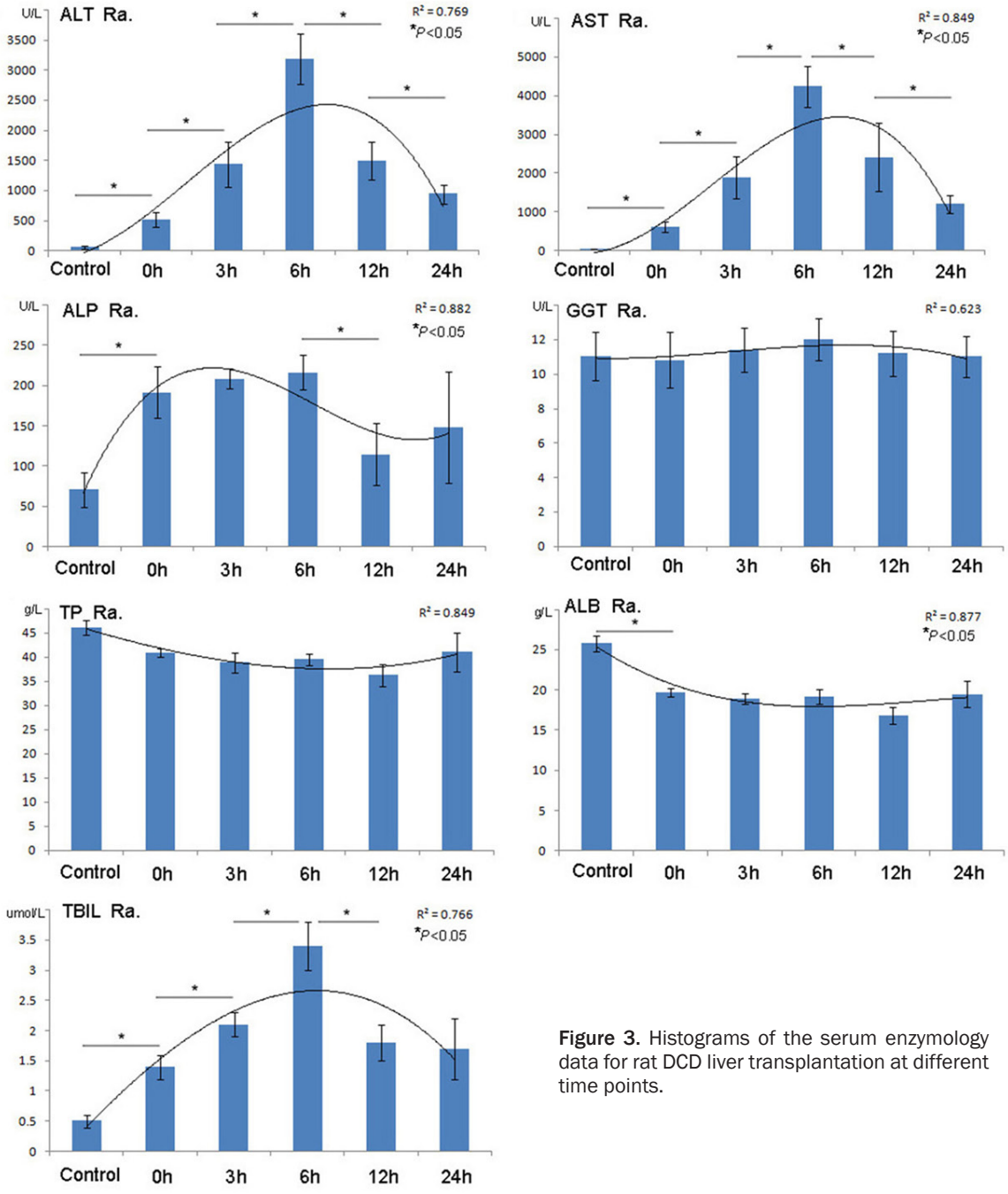

Figure 3. Histograms of the serum enzymology data for rat DCD liver transplantation at different time points.

h followed by an anaerobic-reoxygenation culture as described above. After this culture, 10 μL MTS solution per well and then placed in the incubator for another 3 h. The OD value at the 490 nm wavelength in each well was measured with a microplate reader; the above experiment was repeated three times, and the relationship between the experimental group to the control group was performed using a *t*-test. A threshold value of $P < 0.05$ was considered significant.

Results

Rat DCD liver transplantation

Organizational morphology: In the H&E stained samples, the liver tissue structure and cell morphology of the 0-h, 3-h, 6-h, and 12-h groups exhibited no obvious abnormal changes compared with the control. Moreover, no sinusoidal endothelial cell swelling, inflammatory cell infil-

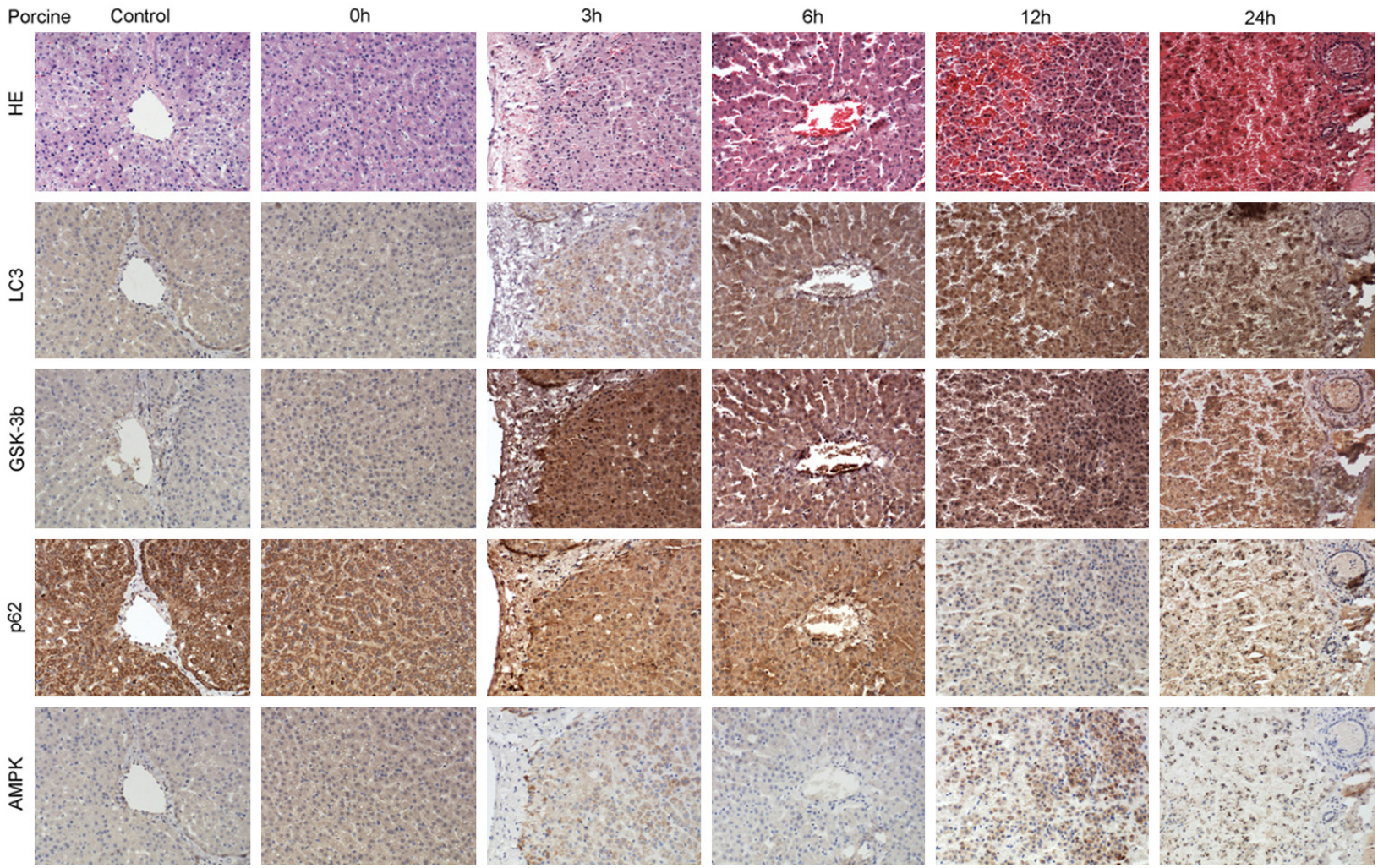

Figure 4. Overall changes in H&E staining and immunohistochemical staining at different time points after liver transplantation (×200).

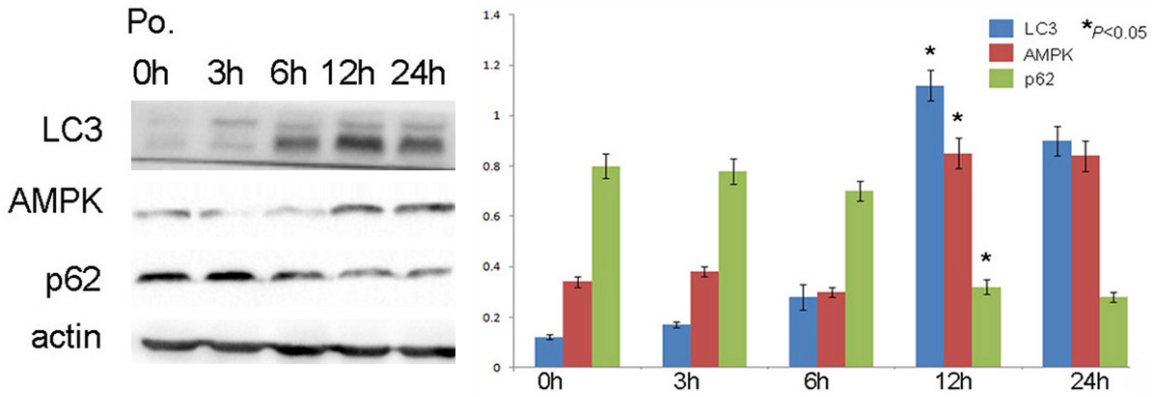

Figure 5. Western Blot detection of LC3, p62, and AMPK expression in the liver. The expression of LC3, p62, and AMPK in the 12 h group was significantly different from the other groups. *P < 0.05 was statistically significant.

tration, or hepatocyte necrosis were observed. In the 24-h group, some of the cytoplasm was stained red and some of the cells had unclear boundaries. Local sinusoidal swelling was accompanied by a small amount of lymphocyte infiltration, but no hepatocyte necrosis was observed, as shown in **Figure 1**. **Figure 1** demonstrates that with a prolonged reperfusion time, the expression of LC3 gradually increased and peaked at 6 h after the operation compared to 0 h ($P < 0.05$). The expression of p62 was significantly down-regulated at 6 h postoperatively compared to 0 h ($P < 0.05$). These findings indicated that hepatocyte autophagy was significantly increased at 6 h postoperatively. The expression of GSK-3β and AMPK was gradually increased and reached a peak at 6 h postoperatively compared to 0 h ($P < 0.05$). Increased expression of GSK-3β and AMPK was associated with enhanced hepatocyte autophagy.

HE: Compared with the control group, the liver tissue structure and cell morphology were not significantly altered in the 0 h-12 h groups. The cytoplasm of the local liver cells was slightly stained red in the 24 h group, and the sinusoids were slightly dilated and devoid of significant cell necrosis. LC3: Compared with the control group, the 0 h group was negative, the LC3 expression gradually increased in the 3 h group, expression peaked in the 6 h group, and expression decreased in the 12 h and 24 h groups. p62: The 0 h group and control group exhibited a high expression, with no significant difference between the two groups. The expression in the 3 h group decreased and the expression in the 6 h group was the lowest. GSK-3β: Compared with the control group, the 0 h and 3 h groups exhibited weak levels of expression, and it peaked in the 6 h group, and decreased in the 12 h and 24 h groups. AMPK: The 0 h and control groups were negative, expression was significantly increased and peaked at 6 h, expression decreased slightly in the 12 h group, and the 24 h group was negative.

Western blot analysis of the expression of LC3, p62, and AMPK in the liver: The expression of LC3 gradually increased from 0 h to 6 h after the operation, and the 6 h group was significantly higher than that of the other groups; the expression of p62 gradually decreased, and it was significantly lower in the 6 h group compared to the other groups, indicating that cellular autophagy increased gradually and there was autophagy flux.

From 0 h to 6 h after operation, the expression of AMPK gradually increased, and peaked at 6 h. AMPK expression increased consistent with the enhancement of autophagy, as shown in **Figure 2**.

Serum enzymology: With the prolongation of reperfusion time, the values of ALT, AST, ALT, and TBIL gradually increased, peaked at 6 h, and subsequently decreased. The changes in GGT, TP, and ALB in each group were not statistically different, as shown in **Figure 3**.

With the extension of reperfusion time, the ALT, AST, ALT and TBIL values gradually increased, and peaked at 6 h. There was no significant difference in the changes of GGT, TP, and ALB

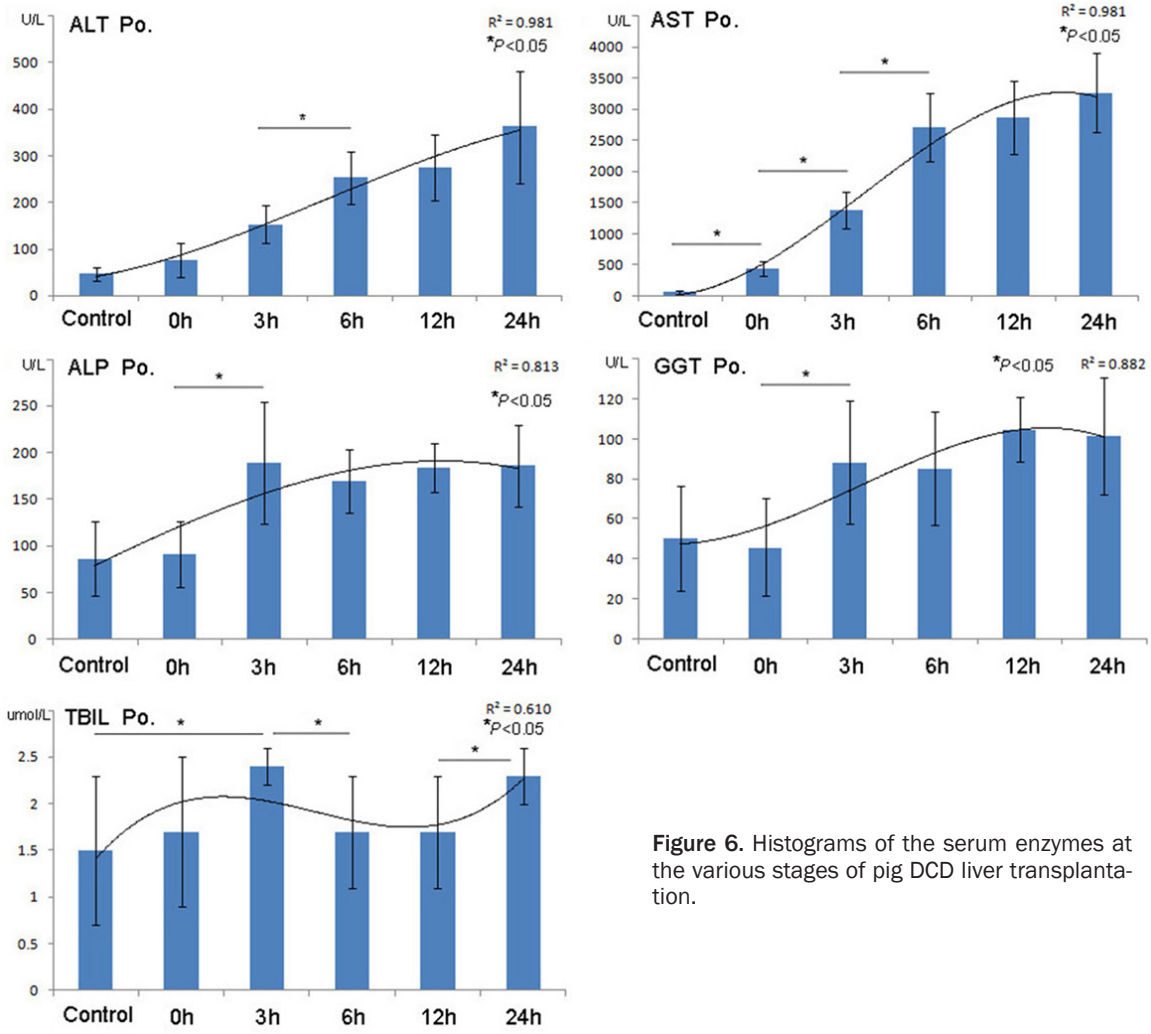

Figure 6. Histograms of the serum enzymes at the various stages of pig DCD liver transplantation.

among the groups. R^2 is the degree of fitness; $*P < 0.05$ represents statistical significance.

Pig DCD liver transplantation test indicators

Histomorphology evaluated by H&E and immunochemical staining: In the H&E-stained samples, compared with the controls, there was no significant change in the liver tissue in the 0 h and 3 h groups. In the liver tissue of the 6 h group, only a few hepatocytes surrounding the portal area were moderately stained red, and most of the liver cells and sinusoidal endothelial cells did not change significantly. In the 12 h group, hepatic sinusoidal dilatation was obvious. Most of the hepatocytes in the portal area and central venous area displayed red staining of the cytoplasm, expansion and congestion of the sinusoids, slight swelling of the sinus endothelium, and significant changes in the portal area. In the 24 h group, hepatocellular necrosis was heavier and bridging necrosis appeared from the portal area to the central venous area; hepatocyte necrosis was observed between the two portal areas and between the two central veins; the cytoplasm was stained red; and the nuclear condensation was deeply stained; part of the cell membrane had ruptured, and the boundaries between the cells were not clear. The hepatic sinusoids were dilated and seriously, congested and the sinus endothelium was significantly swollen with lymphocyte infiltration in the liver tissue, as shown in **Figure 4**.

As shown in **Figure 4**, in the immunohistochemically stained samples, as the reperfusion time was prolonged, the expression of LC3 gradually increased, peaked at 12 h after surgery, and decreased at 24 h. The expression of p62 was significantly down-regulated at 12 h postopera-

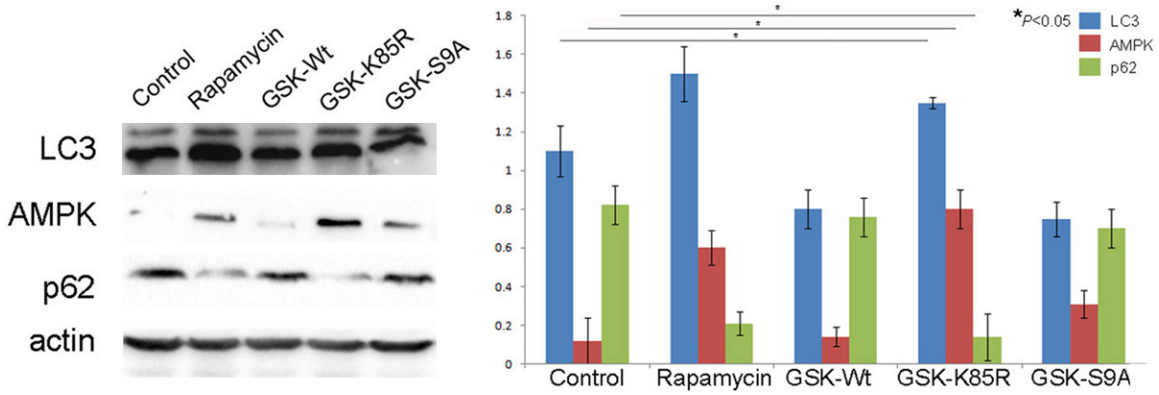

Figure 7. Western blot detecting the effect of different functions of GSK-3β on the expression of LC3, p62, and AMPK in L02 hepatocytes.

tively, indicating that hepatocyte autophagy was significantly enhanced at this time point. The expression of GSK-3β and AMPK increased gradually and peaked at 12 h after surgery. Increased GSK-3β and AMPK expression were associated with enhanced hepatocyte autophagy. All of the above findings were statistically significant ($P < 0.05$).

H&E staining: compared with the control, the 0 h and 3 h groups did not exhibit any significant changes in the microscope; the 6 h group displayed only a small number of hepatocytes around the portal area, which was slightly red-stained. Most of the liver cells and sinusoidal endothelial cells did not change significantly. In the 12 h group, the hepatic sinusoids were significantly dilated, most of the hepatocytes in the portal, the central venous areas exhibited red staining of the cytoplasm, expansion and congestion of the sinuses, and moderate swelling of the sinus endothelium. Changes in the portal sinus were more pronounced. In the 24 h group, hepatocellular necrosis was severe, bridging necrosis was noted, the cytoplasm was stained red, and pyknosis was deeply stained. Some of the cell membranes were ruptured, the boundaries between the cells were unclear, the hepatic sinusoids were dilated and congested, and the sinusoidal endothelium was significantly swollen with lymphocyte infiltration in the liver tissue. LC3: Compared with the control, the 0 h group was negative, and the expression of LC3 gradually increased in the 3 h and 6 h groups, peaking at 12 h. Since hepatocyte necrosis was severe in the 24 h group, LC3 staining was poor and the expression was decreased. p62: the 0 h group and control exhibited high p62 expression, and there was no significant difference between the two groups. P62 expression was decreased in the 3 h group and expression in the 12 h group was the lowest. p62 staining was poor in the 24 h group as the hepatocyte necrosis in this group was severe. GSK-3β: The expression of GSK-3β in the 0 h group was negative compared with the control, significantly increased in the 3 h and 6 h groups and peaked in the 12 h group. Since the degree of hepatocyte necrosis was heavy in the 24 h group, GSK-3β staining was poor and the expression decreased. AMPK: The 0 h group and control group were negative for AMPK, it was increased in the 3 h and 6 h groups, and peaked in the 12 h group due to the hepatocellular necrosis observed in the 24 h group, in which AMPK staining was poor.

Western blot analysis of the expression of LC3, p62, and AMPK in the liver: LC3 expression gradually increased from 0 h to 12 h after the operation, and in the 12 h group was significantly higher than the other groups. The expression of p62 gradually decreased, and the 12 h group was significantly lower than that of the other groups, indicating that cellular autophagy increases gradually and there is autophagy flux.

In addition, the expression of AMPK gradually increased from 0 h to 12 h after the operation and was highest in the 12 h group. The expression of AMPK increased consistent with the enhanced degree of autophagy, as shown in **Figure 5**.

Serum enzymology: With the extension of the reperfusion time, the ALT, AST, and GGT values

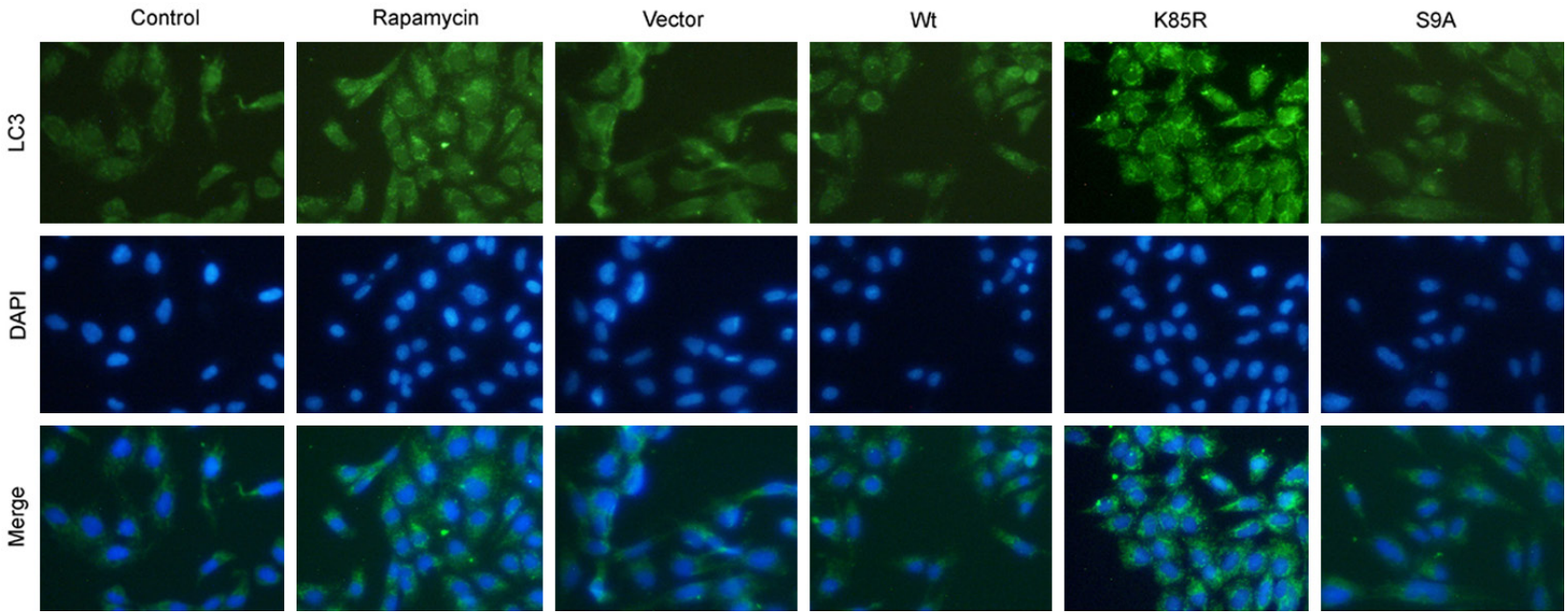

Figure 8. Immunofluorescence was used to test the effect of the autophagy activator, as well as the different functions of GSK-3β on LC3 expression in L02 hepatocytes. The autophagy activator and transfected GSK-3β-K85R could up-regulate the expression of LC3 in the cytoplasm of L02 cells. When transfected with GSK-3β-Wt or GSK-3β-S9A, the expression of LC3 decreased in the L02 cells.

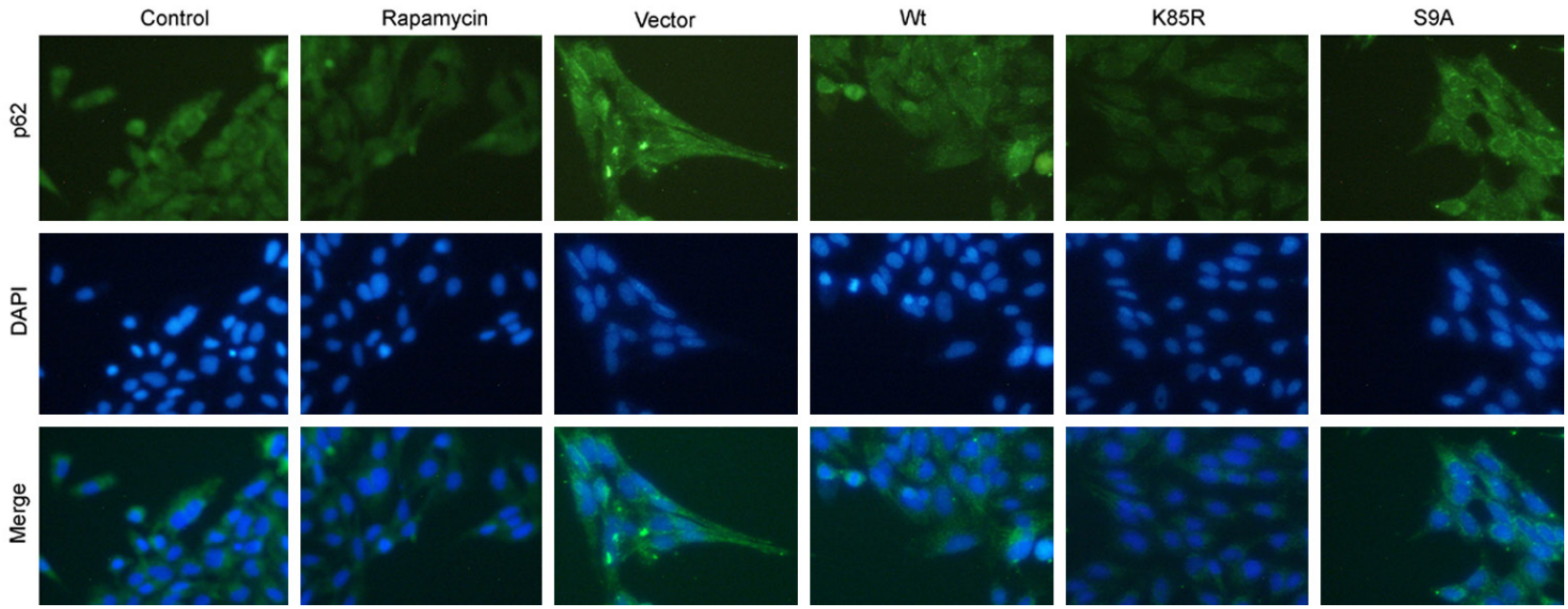

Figure 9. Immunofluorescence was used to identify the effect of the autophagy activator and different functions of GSK-3β on p62 expression in L02 liver cells. The autophagy activator and transfection of GSK-3β-K85R significantly reduced the expression of p62 in the cytoplasm of L02 cells.

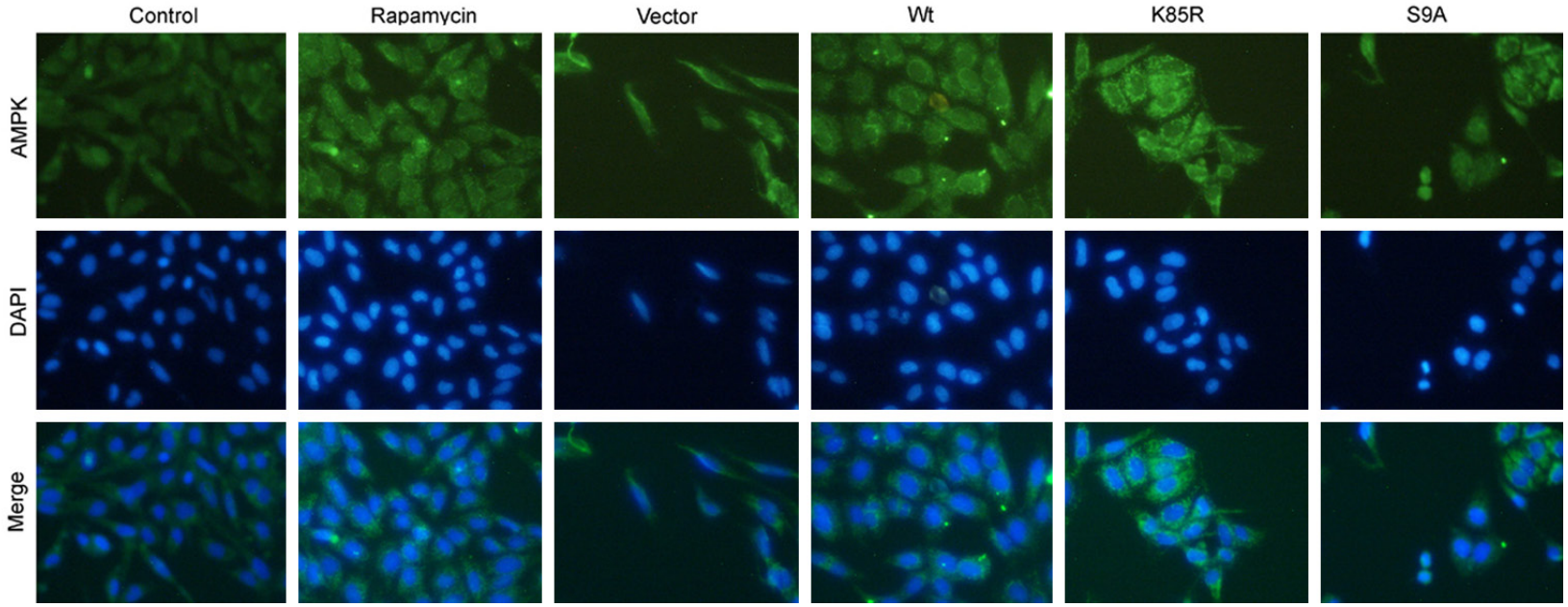

Figure 10. Immunofluorescence revealed the effect of the autophagy activator and different functions of GSK-3β on AMPK expression in L02 hepatocytes. Autophagy activator and transfection of GSK-3β-K85R significantly increased the expression of AMPK in the cytoplasm of L02 cells, while transfection with GSK-3β-Wt or GSK-3β-S9A was associated with decreased AMPK expression in L02 cells.

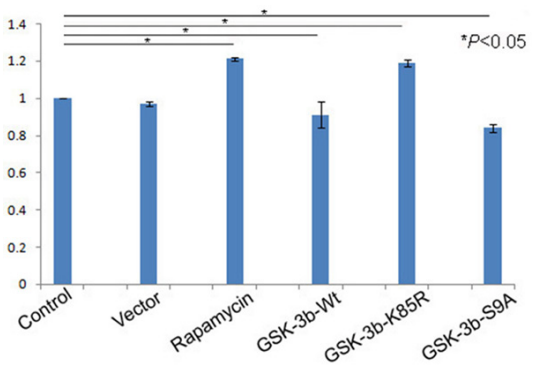

Figure 11. The effect of different GSK-3β functions on the activity of human liver L02 cells.

gradually increased and peaked at 24 h, as shown in **Figure 6**.

Changes in the ALP and TBIL between 3 h, 6 h, 12 h, and 24 h was not statistically different, as shown in **Figure 6**. As the reperfusion time was extended, the ALT, AST, and GGT values gradually increased and peaked at 24 h. At 3 h, 6 h, 12 h, and 24 h, there was no statistical difference in the changes for ALP and TBIL. R^2 is the degree of fitness; $*P < 0.05$ was considered statistically significant.

Different functions of GSK-3β affect the expression of LC3, p62, and AMPK in L02 hepatocytes: Western blot detection of autophagy-related protein expression

In the GSK-3β-K85R group, LC3 and AMPK expression in hepatocytes was up-regulated, whereas p62 expression was down-regulated. In addition, autophagy flux appeared, indicating that GSK-3β-K85R can increase hepatocyte autophagy. However, the expressions of LC3 and AMPK in the GSK-3β-Wt and GSK-3β-S9A groups were down-regulated, while the expression of p62 did not exhibit any obvious changes. No autophagy flux was present, indicating that GSK-3β-Wt and GSK-3β-S9A had no significant effect on hepatocyte autophagy, as shown in **Figure 7**.

The expression of LC3, p62, and AMPK in the autophagy activator and GSK-3β-K85R groups was significantly different from that in the other groups. $*P < 0.05$ is considered significant.

Immunofluorescence detection of protein expression indicating autophagy: LC3 and AMPK expression in the hepatocytes of the GSK-3β-K85R group was up-regulated while the expression of p62 was down-regulated. Autophagy flux appeared, indicating that GSK-3β-K85R can increase hepatocyte autophagy. However, the expressions of LC3 and AMPK in the GSK-3β-Wt and GSK-3β-S9A groups were down-regulated whereas the expression of p62 did not change obviously. There were no signs of autophagy flux, indicating that GSK-3β-Wt and GSK-3β-S9A had no significant effect on hepatocyte autophagy, as shown in **Figures 8-10**.

The effect of different functions of GSK-3β on L02 hepatocyte activity: Compared with the blank control and blank plasmid, GSK-3β-K85R could enhance the activity of cells, and its effect was similar to the autophagy activator group. In contrast, GSK-3β-Wt and GSK-3β-S9A inhibited cell activity, as shown in **Figure 11**. Autophagy activators and GSK-3β-K85R could significantly enhance L02 cell activity. $*P < 0.05$.

Discussion

Thermal ischemic injury is the primary cause of organ damage in DCD, and methods used to evaluate the quality of such organs and in vitro repair is a trending issue in transplantation research. To study the pathophysiological process of DCD liver transplantation and the functional changes of a transplanted liver, researchers have established different models of animal DCD liver transplantation [6-8, 19].

In this study, we successfully implemented rat and porcine DCD liver transplantation by combining both the literature and our own innovative practice [12-14, 20]. To better observe the pathologic morphology and biochemical indexes changes, study mechanisms, and to guide clinical practice, we also selected small and large animals as research objects in liver transplantation studies.

The DCD liver transplantation model in this study mainly simulates Maastricht type III DCD. According to the 2009 guidelines for the acquisition and transplantation of organ donation for controlled cardiac death following the recommendations of the American Society of Transplant Surgeons (ASTS) [21], for DCD liver transplantation, when the actual warm ischemia time exceeds 20-30 min or the total warm ischemia time exceeds 30-40 min, the incidence of

postoperative complications is significantly higher. Therefore, in this experiment, the warm ischemia time of the liver transplantation model was 30 min in order to maximize thermal ischemia injury and ensure that the donor liver was available. The experimental results demonstrate that the animal DCD liver transplantation model was successfully established.

At present, there are few reports investigating the role of cellular autophagy in organ transplantation and the conclusions are inconsistent [22-25]. Therefore, in liver transplantation, the role of autophagy in liver IRI and how it changes during IRI need in-depth study.

GSK-3β is a key kinase that determines cellular fate and it is widely present in mammalian eukaryotic cells [9-11]. If GSK-3β can improve the IRI by regulating hepatocyte autophagy, then GSK-3β can be used as a target to regulate the survival of damaged hepatocytes.

The methods used to identify autophagy primarily include detecting the expression of LC3 and p62 and observing the appearance of the autophagosome under a microscope. LC3-II is a marker of autophagy, for which the expression is proportional to the number of autophagosomes. Therefore, LC3 is widely used to monitor autophagy [26, 27]. p62 is a ubiquitin-binding protein involved in the degradation of the ubiquitin-proteasome system (UPS) and the autophagy-lysosome system. Moreover, since p62 aggregates when autophagy is inhibited, and is reduced when autophagy induced, it is an accurate reflection of the presence of autophagy flux [26, 28-30].

In this study, DCD-grafted liver tissues were collected to analyze the expression of the autophagy markers, LC3, p62, GSK-3β, and AMPK at 0, 3, 6, 12, and 24 h following portal vein blood transfusion. Our results showed that hepatocyte autophagy was significantly enhanced as perfusion was prolonged. The peak of LC3 and MAPK expression in rats was at 6 h post-transplantation. In addition, the expression of LC3 and MAPK peaked at 12 h post-transplantation in pigs. With the extension of reperfusion time, the expression of GSK-3β was also up-regulated and the statistical analysis of the two was related. We noted GSK-3β to be a multifunctional serine/threonine protein kinase whose activity was primarily regulated by specific phosphorylation sites. Phosphorylation of the Try216 site increases kinase activity, whereas kinase activity is inhibited when there is phosphorylation of the Ser9 site, which is more powerful. In this experiment, we found that AMPK expression gradually increased with the extension of reperfusion time and was correlated with the degree of autophagy, suggesting that AMPK may be involved in the process of autophagy caused by liver transplantation ischemia-reperfusion.

In the present study, based on the successful implementation of rat and pig DCD liver transplantation, changes in serum enzymology were detected and analyzed. The results showed that with the extension of the reperfusion time, the ALT, AST, and GGT values gradually increased, peaking at 24 h. This increase in serum ALT and AST coincided with the observed enhanced autophagy.

We transfected different functional GSK-3β plasmids with human normal hepatocytes as experimental subjects, as well as hypoxia-reoxygenation cultured hepatocytes to simulate the IRI process. Our previous results demonstrated that with the extension of reperfusion time, the expression of GSK-3β gradually increased in the transplanted liver tissue, which was consistent with the expression of the autophagy marker, LC3. Thus, GSK-3β, AMPK, and autophagy were related. However, the role of GSK-3β in IRI during liver transplantation remains unclear. Since GSK-3β is a kinase with two functional phases (inactive and activated), immunohistochemistry can only reflect the expression of total GSK-3β, since it cannot distinguish between the specific functional phases of upregulated GSK-3β expression or if both forms of GSK-3β are upregulated, or the specific role each of the two GSK-3βs play. For this reason, we constructed GSK-3β plasmids with different functional phases and transfected them into human liver L02 cells. Following hypoxia-reoxygenation culture, we observed changes in autophagy and cell viability. The results showed that transfection with GSK-3β-K85R inhibited the activity of GSK3β, increased the expression of AMPK and LC3, and promoted autophagy in L02 cells. Moreover, transfection with GSK-3β-S9A enhanced GSK3β activity, decreased the expression of AMPK and LC3, and inhibited autophagy in L02 cells. Therefore, only inactive

GSK-3β was able to enhance the activity of hepatocytes, and neither activated nor wild-type GSK-3β could enhance hepatocyte activity. The autophagy activator, rapamycin, has been shown to enhance hepatocyte activity [31-34]. Combining the western blot results with the prolonged time of ischemia and hypoxia, LC3 expression was gradually up-regulated at the same time that p62 expression was down-regulated. This indicates that the hepatocytes displayed both autophagy and autophagy flux. Moreover, while autophagy in the rats peaked at 6 h, autophagy peaked at 12 h in pigs. Furthermore, the expression of AMPK was consistent with the expression of LC3 over time. Therefore, we speculate that GSK-3β may regulate the level of autophagy and cellular activity of L02 hepatocytes through the AMPK-mTOR pathway.

Rapamycin was used in the present study as an activator of cell autophagy to stimulate L02 cells, and cell viability was measured with an MTS assay. We found that the activation of autophagy could enhance the activity of L02 cells, and had a protective effect on L02 cells.

Studies have shown GSK-3β to inhibit cellular proliferation, especially in cell development and tumor formation, as GSK-3β is an important regulatory factor of the Wnt signaling pathway [35]. Combined with the results of this study, we speculate that the use of different functional phases of GSK-3β is required. Inactive GSK-3β appears to reduce liver IRI, promote hepatocyte autophagy, and improve hepatocyte activity; however, in the case of chronic rejection, activated GSK-3β can be used to inhibit vascular endothelial growth and reduce rejection.

Currently, there are an increasing number of studies performing in-depth research of the various autophagy regulatory pathways. Moreover, researchers have found that there are several key proteins associated with autophagy pathways. It is clear that oxygen free radical bursts, an overload of intracellular calcium, and inflammatory reactions are all involved in the occurrence of IRI. Thus, autophagy may be only one mechanism of IRI, and whether there are more pathways involved in the regulation of hepatic DCD autophagy remains to be studied.

Acknowledgements

We acknowledge the work supported by Clinical Study on Expanding Organ Sources and Improving the Quality of Life and Long-term Survival of Transplant Patients (Special Collaboration of Scientific Research in Public Welfare Industry, No. 201302009).

Disclosure of conflict of interest

None.

Address correspondence to: Dr. Yongfeng Liu, Department of Hepatobiliary Surgery of No. 1 Hospital of China Medical University, Nanjingbei Street 155, Shenyang, Liaoning, PR China. Tel: 0086-24-83-283308; E-mail: yfliu@mail.cmu.edu; 469883299@qq.com

References

[1] Zaouali MA, Boncompagni E, Reiter RJ, Bejaoui M, Freitas I, Pantazi E, Folch-Puy E, Abdennebi HB, Garcia-Gil FA and Rosello-Catafau J. AMPK involvement in endoplasmic reticulum stress and autophagy modulation after fatty liver graft preservation: a role for melatonin and trimetazidine cocktail. J Pineal Res 2013; 55: 65-78.

[2] Degli Esposti D, Sebagh M, Pham P, Reffas M, Pous C, Brenner C, Azoulay D and Lemoine A. Ischemic preconditioning induces autophagy and limits necrosis in human recipients of fatty liver grafts, decreasing the incidence of rejection episodes. Cell Death Dis 2010; 2: e111.

[3] Evankovich J, Zhang R, Cardinal JS, Zhang L, Chen J, Huang H, Beer-Stolz D, Billiar TR, Rosengart MR and Tsung A. Calcium/calmodulin-dependent protein kinase IV limits organ damage in hepatic ischemia-reperfusion injury through induction of autophagy. Am J Physiol Gastrointest Liver Physiol 2012; 303: G189-198.

[4] Cursio R, Colosetti P, Saint-Paul MC, Pagnotta S, Gounon P, Iannelli A, Auberger P and Gugenheim J. Induction of different types of cell death after normothermic liver ischemia-reperfusion. Transplant Proc 2010; 42: 3977-3980.

[5] Wang D, Ma Y, Li Z, Kang K, Sun X, Pan S, Wang J, Pan H, Liu L, Liang D and Jiang H. The role of AKT1 and autophagy in the protective effect of hydrogen sulphide against hepatic ischemia/reperfusion injury in mice. Autophagy 2012; 8: 954-962.

[6] Liu A, Fang H, Dahmen U and Dirsch O. Chronic lithium treatment protects against liver ischemia/reperfusion injury in rats. Liver Transpl 2013; 19: 762-772.

[7] Kang JW, Cho HI and Lee SM. Melatonin inhibits mTOR-dependent autophagy during liver ischemia/reperfusion. Cell Physiol Biochem 2014; 33: 23-36.

[8] Fang H, Liu A, Dahmen U and Dirsch O. Dual role of chloroquine in liver ischemia reperfusion injury: reduction of liver damage in early phase, but aggravation in late phase. Cell Death Dis 2013; 4: e694.
[9] MacDonald BT, Tamai K and He X. Wnt/beta-catenin signaling: components, mechanisms, and diseases. Dev Cell 2009; 17: 9-26.
[10] McCubrey JA, Davis NM, Abrams SL, Montalto G, Cervello M, Basecke J, Libra M, Nicoletti F, Cocco L, Martelli AM and Steelman LS. Diverse roles of GSK-3: tumor promoter-tumor suppressor, target in cancer therapy. Adv Biol Regul 2013; 54: 176-196.
[11] Takahashi-Yanaga F and Sasaguri T. GSK-3beta regulates cyclin D1 expression: a new target for chemotherapy. Cell Signal 2008; 20: 581-589.
[12] Cai Q, Fan H, Xiong R and Jiang Y. A rat model of liver transplantation with a steatotic donor liver after cardiac death. Int J Clin Exp Med 2015; 8: 15724-15730.
[13] Czigany Z, Iwasaki J, Yagi S, Nagai K, Szijarto A, Uemoto S and Tolba RH. Improving research practice in rat orthotopic and partial orthotopic liver transplantation: a review, recommendation, and publication guide. Eur Surg Res 2015; 55: 119-138.
[14] Qing ZS, Zhang XS, Gao CC, Liu WD, Xia TF, Wu K and Pang LQ. Protective effect of ischemia preconditioning on ischemia-reperfusion injury in rat liver transplantation. Genet Mol Res 2015; 14: 3018-3025.
[15] Bruinsma BG, Berendsen TA, Izamis ML, Yeh H, Yarmush ML and Uygun K. Supercooling preservation and transplantation of the rat liver. Nat Protoc 2015; 10: 484-494.
[16] Chen MH, Liu TW, Xie L, Song FQ, He T, Zeng ZY and Mo SR. A simpler cardiac arrest model in rats. Am J Emerg Med 2007; 25: 623-630.
[17] Kamada N and Calne RY. Orthotopic liver transplantation in the rat. Technique using cuff for portal vein anastomosis and biliary drainage. Transplantation 1979; 28: 47-50.
[18] Rhee JY, Alroy J and Freeman RB. Characterization of the withdrawal phase in a porcine donation after the cardiac death model. Am J Transplant 2011; 11: 1169-1175.
[19] Nowak G, Ungerstedt J, Wernerman J, Ungerstedt U and Ericzon BG. Metabolic changes in the liver graft monitored continuously with microdialysis during liver transplantation in a pig model. Liver Transpl 2002; 8: 424-432.
[20] Shi Y, Zhang W, Deng YL, Zhang YM, Zhang QS, Zhang WY, Zheng H, Pan C and Shen ZY. Magnetic ring anastomosis of suprahepatic vena cava: novel technique for liver transplantation in rat. Transpl Int 2014; 28: 89-94.
[21] Reich DJ, Mulligan DC, Abt PL, Pruett TL, Abecassis MM, D'Alessandro A, Pomfret EA, Freeman RB, Markmann JF, Hanto DW, Matas AJ, Roberts JP, Merion RM and Klintmalm GB. ASTS recommended practice guidelines for controlled donation after cardiac death organ procurement and transplantation. Am J Transplant 2009; 9: 2004-2011.
[22] Sanchez-Urdazpal L, Gores GJ, Ward EM, Maus TP, Wahlstrom HE, Moore SB, Wiesner RH and Krom RA. Ischemic-type biliary complications after orthotopic liver transplantation. Hepatology 1992; 16: 49-53.
[23] Buis CI, Hoekstra H, Verdonk RC and Porte RJ. Causes and consequences of ischemic-type biliary lesions after liver transplantation. J Hepatobiliary Pancreat Surg 2006; 13: 517-524.
[24] Cursio R and Gugenheim J. Ischemia-reperfusion injury and ischemic-type biliary lesions following liver transplantation. J Transplant 2012; 2012: 164329.
[25] Cursio R, Colosetti P and Gugenheim J. Autophagy and liver ischemia-reperfusion injury. Biomed Res Int 2015; 2015: 417590.
[26] Berezowska S and Galvan JA. Immunohistochemical Detection of the autophagy markers LC3 and p62/SQSTM1 in formalin-fixed and paraffin-embedded tissue. Methods Mol Biol 2017; 1560: 189-194.
[27] Wu ZZ, Zhang JJ, Gao CC, Zhao M, Liu SY, Gao GM and Zheng ZH. Expression of autophagy related genes mTOR, Becline-1, LC3 and p62 in the peripheral blood mononuclear cells of systemic lupus erythematosus. Am J Clin Exp Immunol 2017; 6: 1-8.
[28] Wang Y, Zhu WG and Zhao Y. Autophagy substrate SQSTM1/p62 regulates chromatin ubiquitination during the DNA damage response. Autophagy 2017; 13: 212-213.
[29] Watanabe Y, Tsujimura A, Taguchi K and Tanaka M. HSF1 stress response pathway regulates autophagy receptor SQSTM1/p62-associated proteostasis. Autophagy 2017; 13: 133-148.
[30] Feng L, Zhang J, Zhu N, Ding Q, Zhang X, Yu J, Qiang W, Zhang Z, Ma Y, Huang D, Shen Y, Fang S, Yu Y and Wang H. Ubiquitin ligase SYVN1/HRD1 facilitates degradation of the SERPINA1 Z variant/alpha-1-antitrypsin Z variant via SQSTM1/p62-dependent selective autophagy. Autophagy 2017; 13: 686-702.
[31] Nagata J, Matsui M and Tabata Y. Intracellular release of rapamycin from poly (lactic acid) nanospheres modifies autophagy. J Biomater Sci Polym Ed 2016; 27: 1291-1302.
[32] Campos T, Ziehe J, Fuentes-Villalobos F, Riquelme O, Pena D, Troncoso R, Lavandero S,

Morin V, Pincheira R and Castro AF. Rapamycin requires AMPK activity and p27 expression for promoting autophagy-dependent Tsc2-null cell survival. Biochim Biophys Acta 2016; 1863: 1200-1207.

[33] Li Y, Liu F, Wang Y, Li D, Guo F, Xu L, Zeng Z, Zhong X and Qian K. Rapamycin-induced autophagy sensitizes A549 cells to radiation associated with DNA damage repair inhibition. Thorac Cancer 2016; 7: 379-386.

[34] Martinez-Cisuelo V, Gomez J, Garcia-Junceda I, Naudi A, Cabre R, Mota-Martorell N, Lopez-Torres M, Gonzalez-Sanchez M, Pamplona R and Barja G. Rapamycin reverses age-related increases in mitochondrial ROS production at complex I, oxidative stress, accumulation of mtDNA fragments inside nuclear DNA, and lipofuscin level, and increases autophagy, in the liver of middle-aged mice. Exp Gerontol 2016; 83: 130-138.

[35] Blankesteijn WM, van de Schans VA, ter Horst P and Smits JF. The Wnt/frizzled/GSK-3 beta pathway: a novel therapeutic target for cardiac hypertrophy. Trends Pharmacol Sci 2008; 29: 175-180.